Preliminary Analysis for Marine Application of Flettner Rotors

A. De Marco*, S. Mancini*, C. Pensa*

***University of Naples "Federico II", Italy,** agostino.demarco@unina.it, simone.mancini@unina.it, claudio.pensa@unina.it

Abstract

The paper presents Unsteady Reynolds Average Navier Stokes (U-RANS) simulations for 3D flow past a full-scale rotating cylinder, known as Flettner Rotor (FR). The U-RANS simulations are performed using the commercially available flow simulation software CD-Adapco STAR CCM+. A preliminary 2D study was conducted to set-up a numerical model using a moving mesh technique; this analysis was directed to define suitable domain shape and dimension, time-step and grid-resolution.

The further 3D simulations were performed to evaluate in deep the influence of some of the main parameters on the effectiveness of the rotors; in particular the Spin Ratio, i.e. the ratio of circumferential-cylinder-velocity-to-free stream-velocity (SR) and the effect of the endplates (EP) also called Thom disk.

The functioning characteristic of the device has been predicted by lift and drag coefficients for various rotation rates.

The selected dimensions of the cylinder and the chosen range of design parameters are similar to those of a real installation on board, therefore the Rn obtained (1.3 - 5.0 E+06) are quite close to the real values and significantly higher than the ones used by other authors in literature. The high-Rn simulations presented here were onerous in terms of computing time but they have proven to be very helpful to evaluate the reliability of numerical studies of large- and small-scale models. Data obtained ware compared with experimental trends found in the literature.

The final task of the research is the assessment of FR concept as an effective naval propeller, therefore the downstream flow field has been closely studied in order to obtain simple and reliable indications on the effective positioning of multiple cylinders on the ship. This study is based on several visualizations of the rotating cylinder wake and takes into account the trailing vortices extinction distance.

Consistently with the point of evaluating the necessity and the feasibility of high Rn simulations, a cost-and-benefit analysis has been enabled showing the computational times of the simulations and numbers of CPUs used.

Keywords: Unconventional ship propulsion**,** Flettner Rotor, Magnus Effect, Full Scale CFD Analysis

1. Introduction

Flettner Rotors are spinning cylinders, which produce fluid dynamic lift using the Magnus Effect. The Magnus force can be many times greater in magnitude than the wing lifting force, given the same projected area and dynamic air pressure.

Anton Flettner, a German Aviation Engineer, used spinning cylinders for the first time as a ship's propulsion system in the 1920's. In Fig. 1 is shown the first Flettner rotor ship designed and built in 1925-26 to improve to the conventional sailing rigs. Further commercial development did not take place before the 21st Century, when the increasing fuel prices and a growing sensibility to the necessity of an anti-pulling policy, the potential of the Flettner rotor is nowadays being seriously examined.

Fig. 1. Buckau (first Flettner's ship) and E-Ship 1 (Enercon Wind Company)

In 2010, Enercon, a wind energy company, launched a Flettner powered cargo ship, named E-Ship 1, and shown in Fig. 1. On the E-Ship 1 the rotors are used to assist the diesel engine, and cut fuel consumption by approximately 30% (as declared by the Enercon). The E-Ship 1 is in current use and has been recounted to cover more than 17,000 sea miles through various waters and with no mention of particular problems about Flettner rotors (Enercon, 2013).

2. Literature Overview

The first systematic study on FR was (Reid E. G., 1924) carried out at the Langley Field NACA Laboratory. In the most complete experimental work on rotating cylinders (Thom A., 1934) the effects of Rn, surface condition, aspect ratio and endplates (EP) disks were investigated and the behaviour of the FR in terms of lift, drag, and torque coefficients was given. In (Swanson W. M., 1961) the physics underpinning the FR was clarified highlighting the nature of the circulation around the rotating cylinder. Recently an experimental and numerical study was described in (Badalamenti C. and Prince S.A., 2008 – Badalamenti C. et al. 2012). With these studies, it was carried out a systematic analysis of the effects of key parameters, but for low Rn (< 1.0 E+05).

The aerodynamic coefficients of an FR depend on various parameters. In this section, the characteristics of a rotating body in cross-flow and the most important parameters are briefly summarized.

2.1. Effect of spin ratio

The aerodynamic characteristics of a FR are mainly influenced by the spin ratio (i.e. the ratio between the circumferential speed of the rotor and the free stream velocity). The flow phenomenology around a circular cylinder is rather complex and consists of tip vortices and an alternate vortex shedding between the rotor sides. It is known that vortex shedding occurs for Rn all the way up to at least Rn =8.0 E+06 (Seifert, 2012). The Strouhal numbers, defined by $St = fD/U$, describe the oscillating flow past a rotating cylinder where f is the frequency of vortex shedding. Low Strouhal number (St < 1.0 E+04) indicates a quasi-steady flow. The Kàrman vortex street is seen for SR = 0 – 2.0. The eddies are formed and shed alternately on two sides of the cylinder. The long eddy formation is for SR = 0 and is considerably shortened for higher SR. Vortex formation and shedding can no longer be seen for SR > 2 and at SR = 3.0 a quasi-steady-state is observable. At SR = 3.5 a second shedding mode was found. In (Mittal S. and Kumar B, 2003) an deep analysis on vortex Shedding is explained.

2.2. Effect of Reynolds number

Swanson (Swanson W. M., 1961) in his work pointed out that lift and drag of a rotating cylinder at SR < 1 show a significant dependency on Rn. The effect is particularly pronounced for the lift at Rn > 6.0 E+04 (with Rn based on the cylinder diameter), this is confirmed by recent study of Gowree and Prince (Gowree E. R. and Prince S. A., 2012). At SR >2.5 and Rn > 4.0 E+04 drag and lift curves have a slightly growing trend as Rn increase.

2.3. Effect of aspect ratio

Relatively to the aspect ratio, the behaviours of a FR and a wing are similar. On the ends of both devices the leakage flows cause a pressure equalization and a vortices generation. Swanson in (Swanson W. M., 1961) concluded in his review paper that the smaller the aspect ratio the smaller the maximum lift obtained and the smaller the velocity ratio at which this maximum is reached. In the same paper Swanson demonstrated that, for very high aspect ratio, lift can reach values higher that the maximum theoretical limit predicted in (Prandtl L., 1925). In Fig. 6 the comparison of these two limit curves is shown.

2.4. Effect of tip geometry

The idea of applying EP to the rotors was suggested in (Prandtl L., 1925). Ten years later Thom in (Thom A., 1934) investigated the effect of large EP with De/D = 3.0. The studies suggest that the EP substantially cause the doubling of the lift at high velocity ratios SR = 2.

In (Badalamenti C. and Prince S A. 2008) it is shown that for a cylinder with AR = 5.1 and diameter ratios ranging from De/D = 1.1 to 3.0, the effects of the increases De/D and AR are similar: a growing trend of lift and a delay of the occurrence of its maximum to higher SR.

The choice of EP size for the best performance was found to be dependent on SR. At low spin ratio, SR = 1, smaller plates generally give lightly smaller drag. For applications at moderate spin ratio, 1 < SR < 3, larger

plates are preferred, so as to delay the increase in induced drag. For high spin ratio applications, SR > 3, smaller plates are again more desirable as the drag quickly approaches a limit, as you can see in Fig. 2.

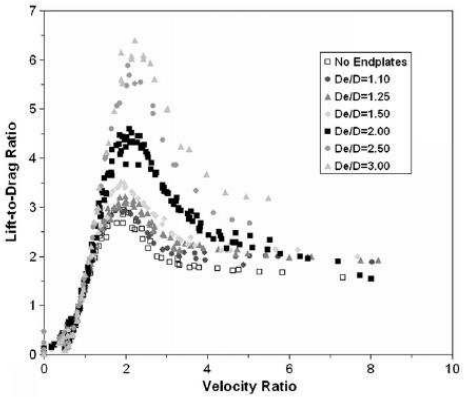

Fig. 2. Effect of EP diameters on lift coefficient (Seifert, 2012)

3. Numerical Setup

3.1. Geometry

The geometry used was taken from the real application of E-Ship 1 by Enercon Company. The cylinder aspect ratio is AR = 3.5 corresponding to a cylinder length of H = 14.0 m and a diameter of D = 4.0 m. EP diameter tested is De/D = 2.0 (Fig. 3).

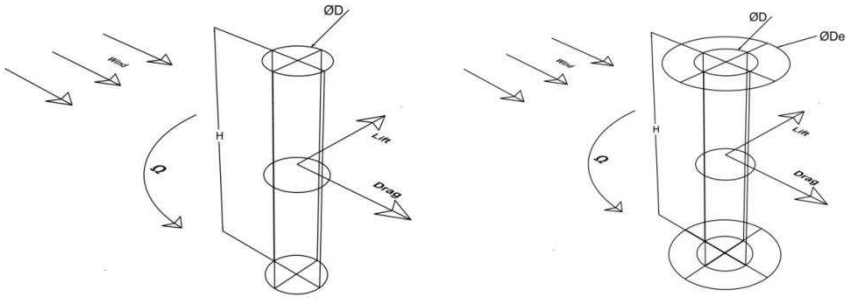

Fig. 3. Rotors geometry with and without end plate and relevant parameters

3.2. Numerical method

The mesh and URANS simulations are performed using the commercially available flow simulation software CD-ADAPCO STAR CCM+ v.8.04. A 3D hybrid grid (unstructured outer grid with embedded structured boundary layer zone) was used. The Solver use an implicit element-based finite volume method. A segregated flow approach with second order upwind discretization of the convective term is used throughout all simulations (User Guide STAR-CCM+ v. 8.04, 2013). For the temporal discretization a first order forward Euler scheme is used (User Guide STAR-CCM+ v. 8.04, 2013). In the calculations the flow is assumed incompressible. Fully turbulent calculations are carried out using the k-ω Shear Stress-Transport (SST) turbulence model (Menter F. R., 1994). Furthermore the rotation of FR in the simulation is obtained by overset mesh methodology with distance-weighted interpolation. All the calculations were performed on the SCoPE Supercomputing Center of the Università degli Studi di Napoli *"Federico II"*. The 2D Analysis were performed using 64 CPUs and the 3D Analysis 120 CPUs.

3.3. Preliminary 2D analysis

To reduce the computational effort the first computations were made in 2D mode to set up the main parameters of simulation as the optimal number of cells, the type of mesh and the size of the computational domain. The characteristics of grids, that have been selected, are shown in Table 1.

Table 1. Details of the grids used

Grid Type	Base Size (m)	Number of Cells
Case A (fine) - polyhedral	3.00	138555
Case B (medium) - polyhedral	4.00	92967
Case C (coarse) – polyhedral	5.00	66258
Case D (medium) - trimmed	4.00	126773

The circular cylinder model for the 2D preliminary investigation has the same diameter of the 3D cylinder analysis. The free-stream velocity is assumed fixed at the value of 10.0 m/s, consequently the Rn, based on the cylinder diameter, is kept constant at 2.55 E+06. The simulation time step is a function of Ω, in fact is necessary to have a maximum crossing a cell for time step. All relevant parameters are resuming on Table 2.

Table 2. Resuming simulation parameters of 2D preliminary analysis

Spin Ratio	Ω (rad/s)	Time step (s)	Iteration for Time Step	Phisical time (s)
0.2	1.0	0.01	35	90
1.0	5.0	0.0025	35	70
2.0	10.0	0.00125	35	70
3.0	15.0	0.000625	35	50
4.0	20.0	0.0003125	35	50

The results obtained in terms of lift and drag coefficients were compared with each other and is observed as:

- the polyhedral mesh is better than the mesh trimmed, since Base Size equal to the number of cells is less;
- the Case C is the best compromise between accuracy of the results and calculation times; in fact for the case A simulation with SR = 4 are required 133 h of calculation using 64 CPUs, instead 68 hours with the same CPUs numbers for Case C.

Finally a Discrete Fourier Transformation (1024 size and using Hanning window) was applied to the time history of lift coefficient in order to identify the frequency of vortex shedding and its Strouhal number. The results of various mesh cases (Fig. 4) are substantially in agreement with what is already discussed in paragraph 2.1.

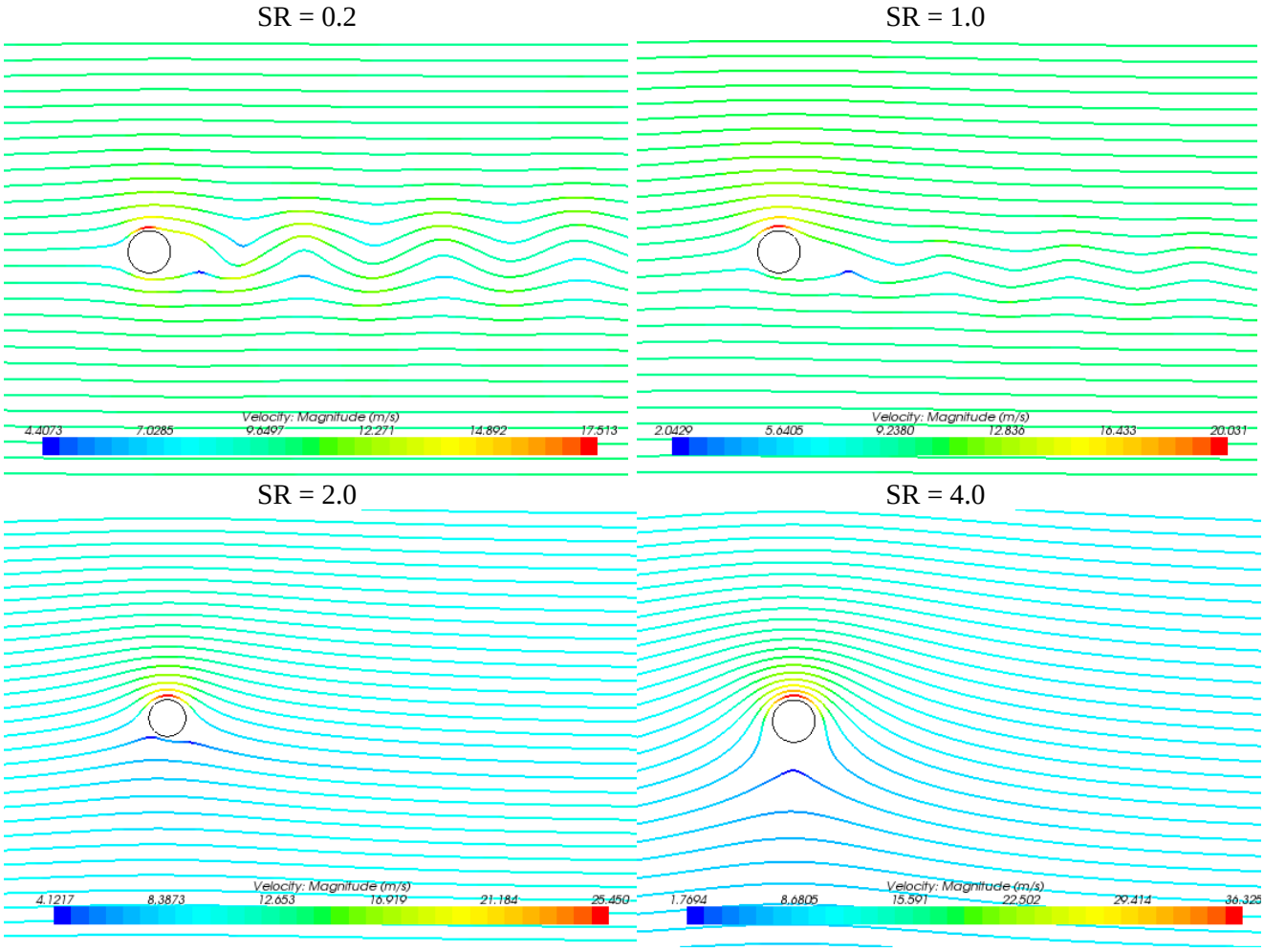

Fig. 4. 2D streamlines for different SR

3.4. Mesh and simulation topology

For 3D analysis has been carried out on basis of 2D results and considerations. The mesh used is polyhedral type mesh Case C (Base Size = 5.0 m), in agreement with the considerations presented in the previous section. The total number of cells is 3482273 for simulations with end plate and 2220672 cells for simulations without end plate. Regular domain is created around the cylinder geometry (Fig. 5). To further make lighter the computational load, only half of the cylinder is modelled and a symmetry plane is used at the mid-length. A velocity inlet boundary condition is set on the front part of the domain with a prescribed velocity. On the rear part of the domain, a pressure outlet boundary condition is imposed with a relative pressure of 0 Pa. On the opposite side of the domain, a symmetry boundary condition is also used. Around the rotor was made a cylindrical area of overlap between the rotating mesh and fix domain, a necessary condition for using the overset mesh methodology.

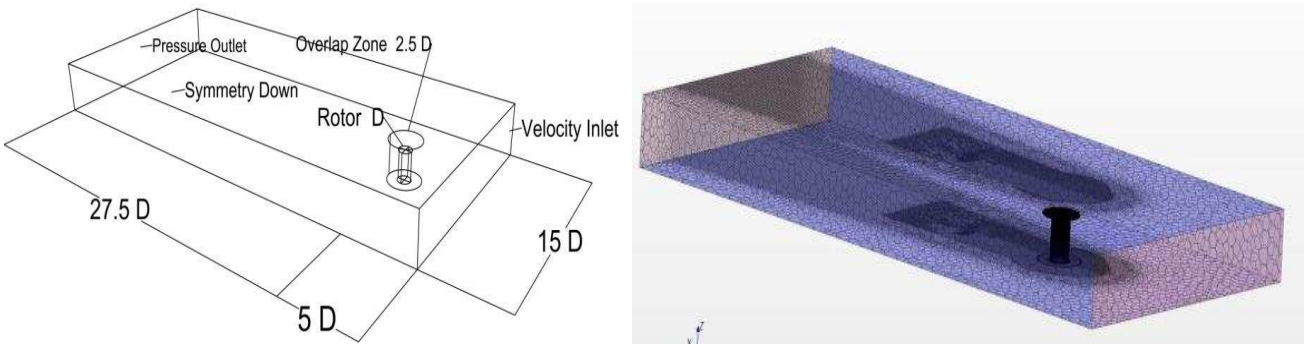

Fig. 5 Mesh and simulation domain with boundary conditions

4. Results and Discussion

Below are the results of 3D simulations for the two configurations tested without end with end plate: (De/D = 2.0), with the same aspect ratio (AR = 3.5).

All the simulations were made keeping cylinder rotation velocity equal to 10 rad/s and the free-stream velocity is variable with what reported in the Table 3 (this condition is closer to the real navigation function). The computational time for each simulation (i.e. for each SR) is estimated at 188 h with 120 CPUs.

Table 3. Resuming simulation parameters of 3D analysis

Spin Ratio	U (m/s)	Re	Time step (s)	Iteration for Time Step	Phisical Time (s)
1.0	20.0	5.11E+06	0.00125	15	30
2.0	10.0	2.55E+06	0.00125	15	30
3.0	6.67	1.70E+06	0.00125	15	30
4.0	5.0	1.28E+06	0.00125	15	30

Graphs show the C_L, C_D and C_L/C_D coefficients obtained from the simulations compared with data available in literature. The C_L, and C_D are according with the equations (1).

$$C_L = \frac{L}{0.5\,\rho\,S_{ref}U^2}, \qquad C_D = \frac{D}{0.5\,\rho\,S_{ref}U^2} \tag{1}$$

To facilitate the analysis of the rotor behaviours, in the next figures the information on the reported simulations are shown.

Table 4

	AR	Rn	EP	De/D	Type of study
Reid (1924)	5.5	7.30 E+04	no	//	experimental
Hoerner and Borst (1975)	n.a.	4.40 E+04	no	//	experimental
Badalamenti and Prince (2008)	5.1	9.60 E+04	yes	2.0	numerical
Bensow & Zhang (2011)	6.0	1.00 E+05	no	//	numerical
Thom (1934)	12.6	1.00 E+04	yes	n.a.	experimental
Present paper; W.EP	3.5	5.11 E+06	yes	2.0	numerical
Present paper; W.out EP	3.5	5.11 E+06	no	//	numerical

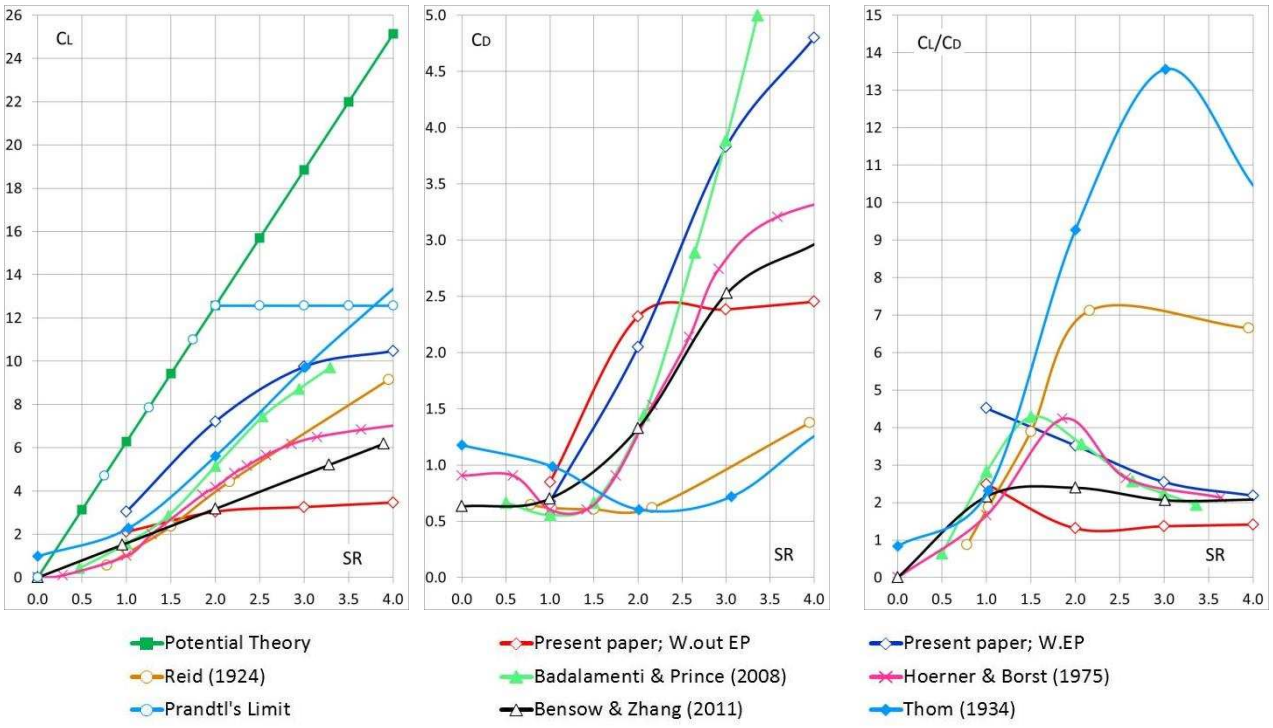

Fig. 6 Aerodynamic coefficients

From the curves represented above is possible to deduce some aspects of the cylinder behaviours evaluated by the various authors.

- The general trend of the C_L and C_D curves is growing with SR value with the partial exception of the cylinders without EP, working at the highest Rn (present study), and of the C_D given by Thom, whose trend, probably, is due to the very high AR.
- All the studies, except the present study that investigate the highest Rn, highlight that the aerodynamic efficiencies C_L/C_D have a maximum in the range SR = 1.5 – 3.0. For the highest Rn the highest values of C_L/C_D haven't been identified and located because they are, probably, in a range lower than that examined.
- In a previous work (Bensow R. and Zhang W., 2011) is mentioned that for Rn between 5.0 E+04 and 1.0 E+05, it is non influent if SR < 2.0. Present study extends this range to Rn = 5.0 E+06.
- Comparing C_L data of the rotors without EP, a good agreement is observable for SR < 1.5. Above this value, the curves diverge. This can depends both on the accuracy of the numerical simulations and on the different AR and Rn of the studied rotors. Nevertheless, observing the quite good similarity of the only two experimental curves, it is possible to presume the need to improve the reliability of the numerical simulations. To confirm this consideration (Bensow R. and Zhang W., 2011) highlight the influence of the numerical solver on the results of the simulations.
- Referring to rotors with EP and comparing the C_L data given by (Badalamenti C. and Prince S A. 2008) and by the present work, a similar trend is shown. The values differ more at low SR and become minimal with SR growing up.

- In a good amount of the SR range the C_D given in this work are higher than those given by (Badalamenti C. and Prince S A., 2008). Observing that for both the rotors De/D = 2.0, it is deducible that the different behaviors are due to the different AR, that are 5.1 and 3.5 for Badalamenti and this work respectively. This conclusion is borne out by the observation that the lower AR the bigger EP (if compared with the cylinder and at constant De/D).
- The C_L and C_D trends above remarked imply a shift of the maximum aerodynamic efficiency (C_L/C_D) to higher SR for higher AR. This trend suggests to use high De/D with low AR cylinders. However it has to consider behavior could be dependent also on the different Rn (9.6 E+04 vs 5.0 E+06).

To facilitate the comprehension in deep of the physic underpinning the behavior of the FR, the vortices created by the cylinders, both with and without the EP, are shown in the next figures. The main aim of these figures is to highlight streamlines and progressive diffusion of the turbulence to evaluate the suitability of the grid domain dimensions.

As made above for the C_L and C_D diagrams, some observations concerning the vortex patterns, shown in Fig.7, are briefly summarized.

- The images highlight the vortices produced by the EP that increase with SR.
- The vortices produced by the cylinders are strongly conditioned by the action of EP that made the cylinder vortices inversely proportional to SR.
- Diversely, the cylinders without EP increase vortices when SR increases.
- The different proportionality to SR of the vortices produced by the EP and by the cylinders implies that the best values of De/D are dependent on SR (as well as on the AR, as above mentioned). This dependency is consistent with data given in Fig. 2.
- Regarding the evaluation of the suitability of the grid domain dimensions, the figures show that the vortices cross the outlet and the top side of the domain mesh. This could be a critical point but it has to note that the intensity of the turbulent kinetic energy of the vortices is quite low in these zones.

The vortices patterns have been identified by the Q criterion shown in (Chakraborty P. et al., 2007). This procedure identifies vortices as iso-surface flow regions with positive second invariant of the velocity gradient tensor ($Q > 0$). The chromatic scale, shown below the Fig. 6, quantifies the turbulent kinetic energy of the vortices.

5. Conclusions

The present study is a preliminary investigation on two matters whose understanding in deep is essential for a real application of FR as ship propulsion system:

1. the physic underpinning these devices with particular attention to the influence of some of the main parameters on the effectiveness of the rotors;
2. the reliability of the numerical simulations to predict the performances of the ship.

With End Plate **SR 1** (a)

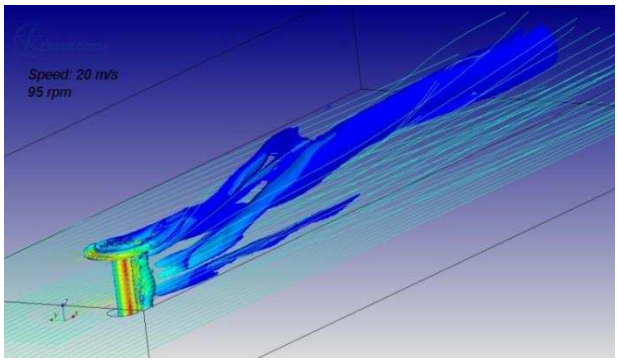

Without End Plate **SR 1** (b)

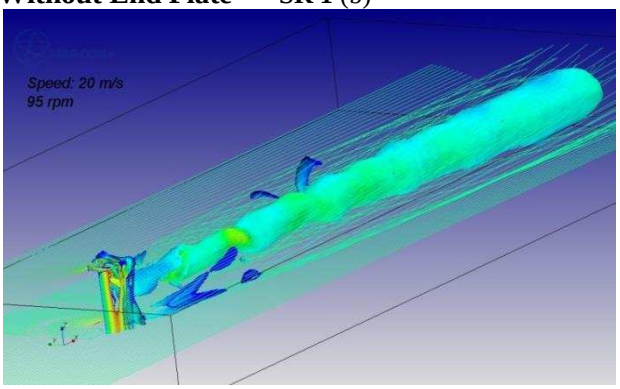

SR 2 (c)

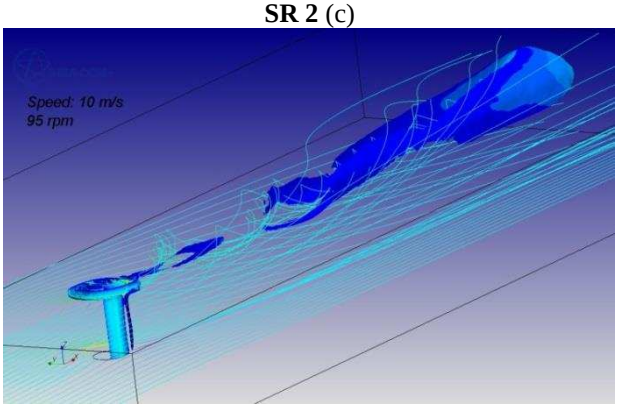

SR 2 (d)

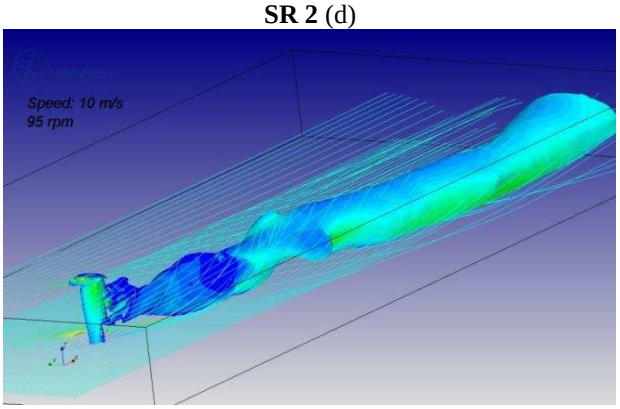

SR 3 (e)

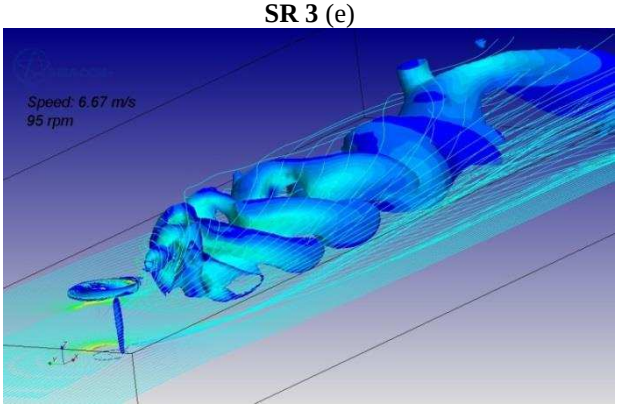

SR 3 (f)

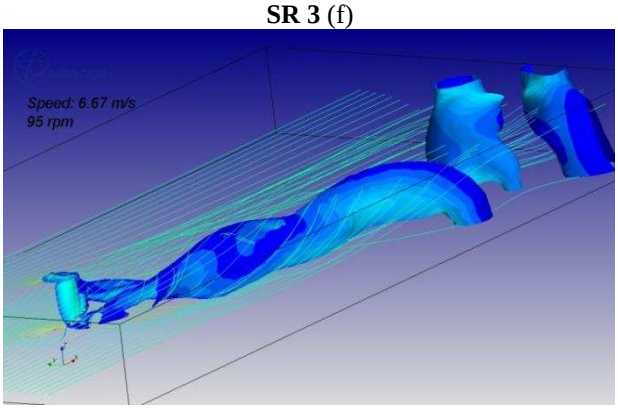

SR 4 (g)

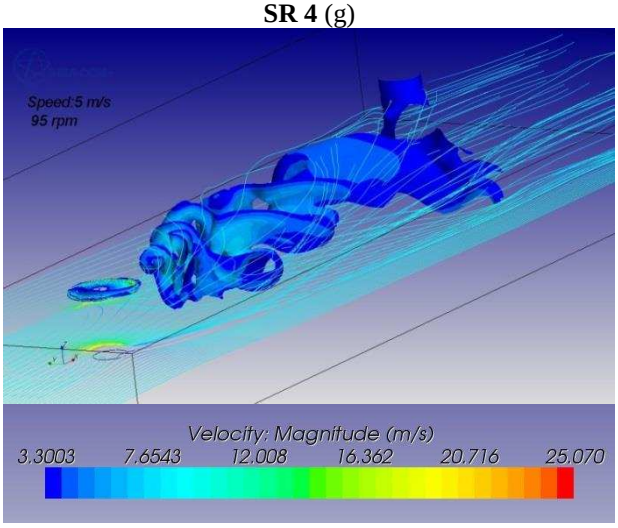

SR 4 (h)

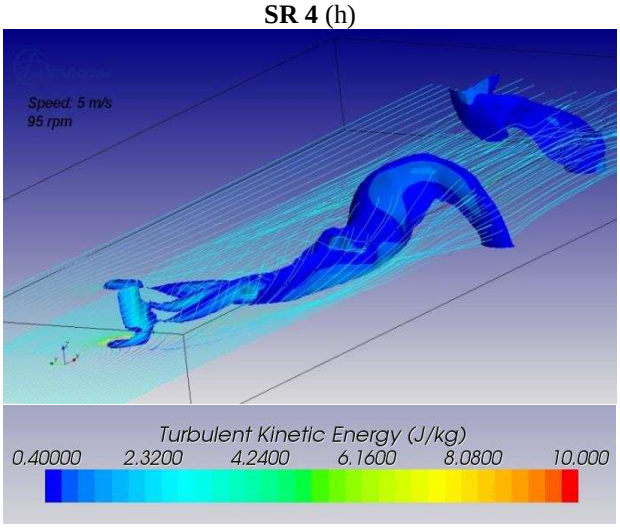

Fig. 7. Streamlines and vortex structures represented by an iso-surface of Q>0. All images are for mid rotor.

1. The comparison between cylinders with and without EP confirmed the higher efficiency of the devices with EP. Furthermore, data obtained highlights that the EP increase dramatically both C_L and C_D and do it proportionally with SR.

For the cylinders with EP, the optimum values of De/D depend on AR and SR with direct and inverse proportionality respectively.

The aerodynamic efficiency, C_L/C_D, is strongly dependant on SR. Nevertheless, considering the FR as ship propulsion system, it has to observe that the highest effective forces depend also on the efficiency of the hall in terms of C_L/C_D (exactly as for any sailing ship) and on the angle between the ship's course and the wind direction.

2. It has been investigated the reliability of simulations carried out with small cylinders and Rn < 10 E+04 instead of Rn near to 5.0 E+06 - typical values for ship applications. This issue has been performed comparing homogeneous data, with and without EP. For both cases the trends of C_L , evaluated at different Rn, are similar but the ranges where the differences are higher are different: high and low SR for cylinders with and without EP respectively.

Regarding the C_D and C_L/C_D, in all the range of SR investigated, this data is substantially more scattered. From the operational point of view it has been accepted that data is quite scattered and not trustworthy for performance predictions. Currently, it has to clarify if this dispersion is due to the accuracy of the numerical simulations or to the low comparability of the studied rotors (or to both the reasons).

The study has shown the high three-dimensional flow also near the symmetry plane (symmetry down surface of the grid domain). This suggests to perform next simulations with the whole cylinder.

Regarding the onerousness of the numerical procedures, the study shown that, currently, the weight of the higher Rn computing are not a minor detail: 188 h with 120 CPUs for each simulation. To give this number full weight, it has been remembered the relatively low reliability of the results.

6. Future works

Before to tackle the contextualization of the FR on a ship, the next steps of the research will study in deep the reliability of the simulations. This will be carried out comparing numerical and experimental data obtained on cylinders strictly identical.

With regard to the onerousness of the high Rn computing, it will be evaluated the sensitivity of the results to the reduction of the main costs factors (domain dimensions and grid density, time step, etc.). This will be important also considering the need to study the whole cylinder due to the high three-dimensional flow.

Finally, it will be studied some devices to improve the effectiveness of the FR as different form of the EP or EP not rotating.

References

Badalamenti, C., and Prince, S A. (2008). The Effects of Endplates on a Rotating Cylinder in Crossflow, Proceedings of the AIAA-7063.

Bensow, R. and Zhang W. (2011). Numerical Simulation of high-Reynolds number flow around Flettner rotors, Proceedings of the NUTTS Southampton, pp. 181-187

Chakraborty, P., Balachandar, S., Adrian, R. J. (2007). Kinematics of Local Vortex Identification Criteria, Journal of Visualization, Vol. 10, No. 2 (2007) 137-140.

Enercon E-Ship 1 A Wind-Hybrid Commercial Cargo Ship (2013). 4th Conference on Ship Efficiency Hamburg.

Gowree, E. R. and Prince, S. A. (2012). A Computational Study of the Aerodynamics of a Spinning Cylinder in a Cross flow of High Reynolds Number, Proceedings of the 28th ICAS, Brisbane, Australia.

Hoerner, S. F. and Borst, H. V. (1975). Fluid-Dynamic Lift, Bricktown, NJ: Hoerner Fluid Dynamics.

Mittal, S. and Kumar, B. (2003). Flow past a rotating cylinder, Journal of Fluid Mechanics, Vol. 476, pp 303-334.

Menter, F R. (1994), Two-Equation Eddy-Viscosity Turbulence Models for Engineering Applications, AIAA Journal , Vol. 32, No. 8, pp. 1598-1605.

Prandtl, L. (1925). The Magnus effect and wind-powered ships, Naturwissenschaften, 13, 1787-1806.

Reid, E. G. (1924). Tests of rotating cylinders, NACA TN 209, pp. 10-11.

Seifert, J. (2012). A review of the Magnus effect in aeronautics, Progress in Aerospace Sciences 55 pp 17–45.

Swanson, W. M. (1961). The Magnus Effect: A Summary of Investigation to Date, ASME Transactions Series D, Journal of Basic Engineering. Vol. 83. pp. 461-470., 1961;

Thouault, N., Breitsamter, N., Seifert, J., Badalamenti, C., Prince, S.A. (2010). Numerical Analysis of a Rotating Cylinder with Spanwise Discs, Proceedings of the 27th ICAS, Nice, France.

Thom A., (1934). Effects of discs on the air forces on a rotating cylinder, Aero. Res. Counc. R&M 1623.

User Guide STAR-CCM+ Version 8.04, 2013.

Symbology and Abbreviations

ρ	Air density	kg/m^3	H	Cylinder length	m
Ω	Angular velocity	rad/s	AR	Aspect Ratio	
BS	Base Size	m	C_L	Lift Coefficient	
D	Drag	N	C_D	Drag Coefficient	
L	Lift	N	EP	Endplate	
Sref	Reference Area	m^2	FR	Flettner Rotor	
U	Free Stream Velocity	m/s	Rn	Reynolds Number	
D	Cylinder Diameter	m	St	Strouhal number	
De	Endplate Diameter	m	SR	Spin Ratio	
n	Revolutions per second	s^{-1}			